SUPPORTING INFORMATION

Lyotropic liquid crystallinity in mixed-tautomer Schiff-base macrocycles

*Jian Jiang, Ronald Y. Dong and Mark J. MacLachlan**

[a] Department of Chemistry, University of British Columbia, 2036 Main Mall, Vancouver, BC, Canada V6T 1Z1. [b] Department of Physics and Astronomy, University of British Columbia, 6224 Agriculture Rd., Vancouver, BC, Canada V6T 1Z1. mmaclach@chem.ubc.ca

Table of Contents

Figures

General Experimental Details

Materials

1-Dodecyl-3-methyl-pyridinium bromide was synthesis by literature methods.[1] Macrocycle **1a** was prepared by a literature procedure.[2] Chloroform, acetonitrile and methanol were dried over oven-activated 4-Å molecular sieves prior to use. $CDCl_3$ and 1,1,2,2-tetrachloroethane-d_2 were obtained from Cambridge Isotope Laboratories, Inc. and dried over oven-activated 4-Å molecular sieves prior to use. Piperidine was obtained from Aldrich and used without further purification.

Instrumentation

^{1}H and ^{13}C NMR spectra were recorded on Bruker AV-400 or AV-600 spectrometer. ^{13}C NMR spectra were recorded using a proton decoupled pulse sequence. 2D COSY and 2D ROESY NMR experiments were performed on a Bruker AV-400 inv spectrometer. UV-vis spectra were obtained on a Varian Cary 5000 UV-vis/near-IR spectrophotometer using a 1 cm cuvette. IR spectra were collected neat in the solid state on a Thermo Nicolet 6700 FT-IR spectrometer equipped with an attenuated total reflectance (ATR) attachment. MALDI-TOF mass spectra were obtained in a dithranol matrix (cast from THF) on a Brüker Biflex IV instrument where spectra were acquired in the positive reflection mode with delay extraction. Elemental analyses (C, H, N) were performed at UBC Microanalytical Services Laboratory. Melting points were obtained on a Fisher-John's melting point apparatus. Liquid crystal textures were observed with an Olympus BX41 polarizing optical microscope equipped with temperature-controlled heating stage (Instec STC200). Differential scanning calorimetry (DSC) experiment was performed on Perkin Elmer Diamond DSC. Light intensity of POM was measured by Newport Optical Power Meter 1830-c with a photodetetor of Newport 818-UV. 2D XRD data were collected on a Bruker D8 DISCOVER GADDS microdiffractometer equipped with an area detector in a rotation method using X-rays generated from a sealed Cu tube, monochromated by a graphite crystal and collimated by a 0.5 mm MONOCAP (λ Cu-Kα =1.54178 Å). 2D X-ray diffraction of the liquid crystal was performed in a 0.1 or 0.2 mm boron-enriched thin-walled capillary tube received from the Charles Supper Company. Powder XRD with Bragg-Brentano diffraction geometry was measured on a Bruker D8 Advance with Cu radiation and a NaI scintillation detector.

Synthesis

Scheme S1. Synthesis of Macrocycles **1a** and **1b**.

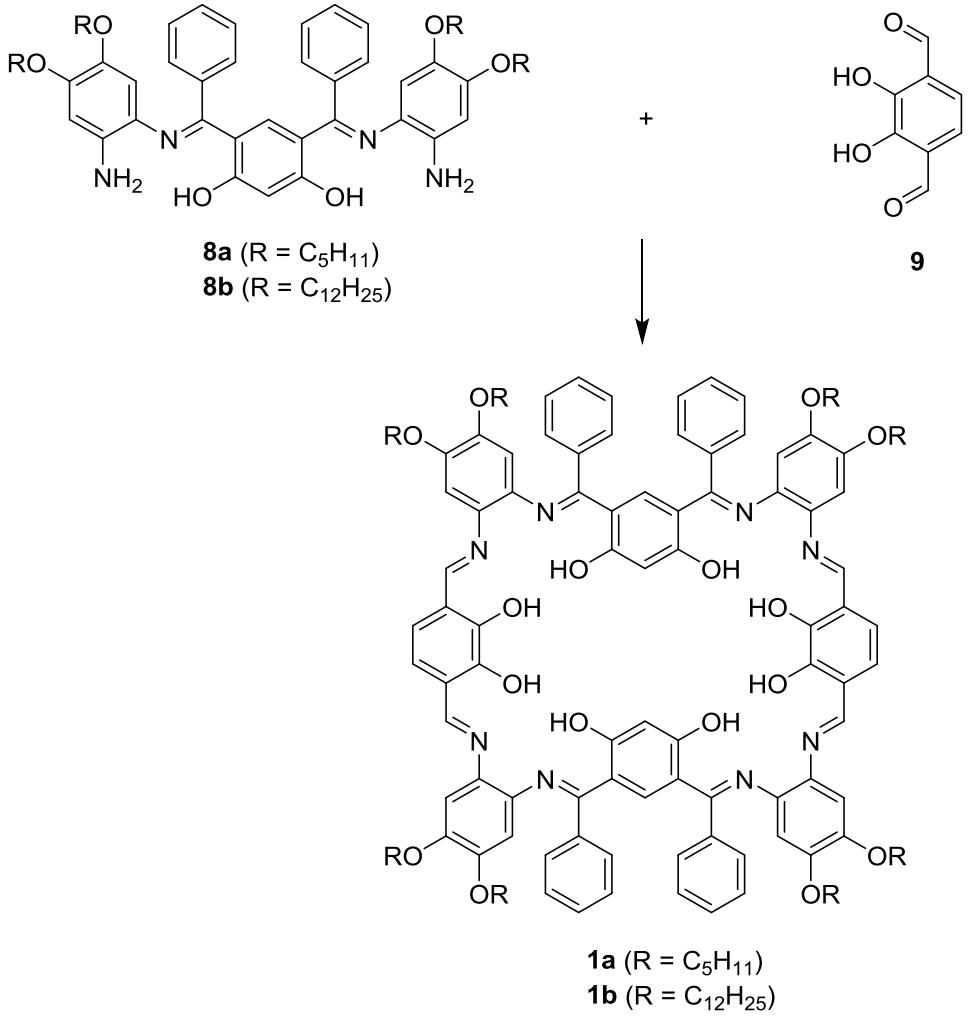

Synthesis of Macrocycle 1b. In a Schlenk flask, compound **8b**[5] (0.28 g, 0.23 mmol), compound **9**[3] (0.038 g, 0.23 mmol), and piperidine (0.04 mL, 0.41 mmol) were dissolved in 60 mL of dry $CHCl_3$:CH_3CN (2:1). The flask was fit with a condenser and the reaction mixture was heated at reflux overnight under N_2. After cooling the reaction mixture to room temperature, the solvent was removed under reduced pressure. The remaining solids were suspended in MeOH and filtered yielding a red powder. The crude product was recrystallized from $CHCl_3$/MeOH giving 0.10 g of dark red macrocycle **1b** (0.036 mmol, 32%).

Data for 1b. ^{1}H NMR (400 MHz, $CDCl_3$): δ 15.20 (s, 4H), 12.89 (s, 4H), 8.35 (s, 4H), 6.95 (m, 26H), 6.61 (s, 4H), 6.52 (s, 2H), 6.15 (s, 4H), 3.92 (t, 8H), 3.58 (t, 8H), 1.80-0.80 (m, 184H). ^{13}C NMR (100.6 MHz, $CDCl_3$): δ 174.2, 169.5, 161.3, 151.2, 148.9, 148.1, 140.9, 135.7, 135.1, 128.9, 129.1, 128.8, 122.0, 121.8, 114.1, 109.2, 106.3, 106.1, 77.7, 71.8, 70.2, 30.2, 29.7, 29.3, 29.1, 29.0, 28.4, 23.5, 23.4, 15.0. UV-Vis (CH_2Cl_2): λmax (ε) = 439 (1.4 x 10^5), 388 (1.6 x 10^5), 338 (1.8 x 10^5), 285 (3.1 x 10^5) nm (L mol^{-1} cm^{-1}). IR (neat) υ = 3010, 2951, 2929, 2856, 1614, 1556, 1305, 1258, 992, 849, 740 cm^{-1}. Anal. Calcd for $C_{176}H_{248}N_8O_{16}$•$5H_2O$: C 74.91, N 3.97, H 9.22; Found: C 74.98, N 4.01, H 9.18. MALDI-TOF MS (dithranol matrix): m/z = 2732.8 $[M+H]^+$. mp = dec. at 250 °C.

Scheme S2. Synthesis of macrocycles **3a** and **3b**

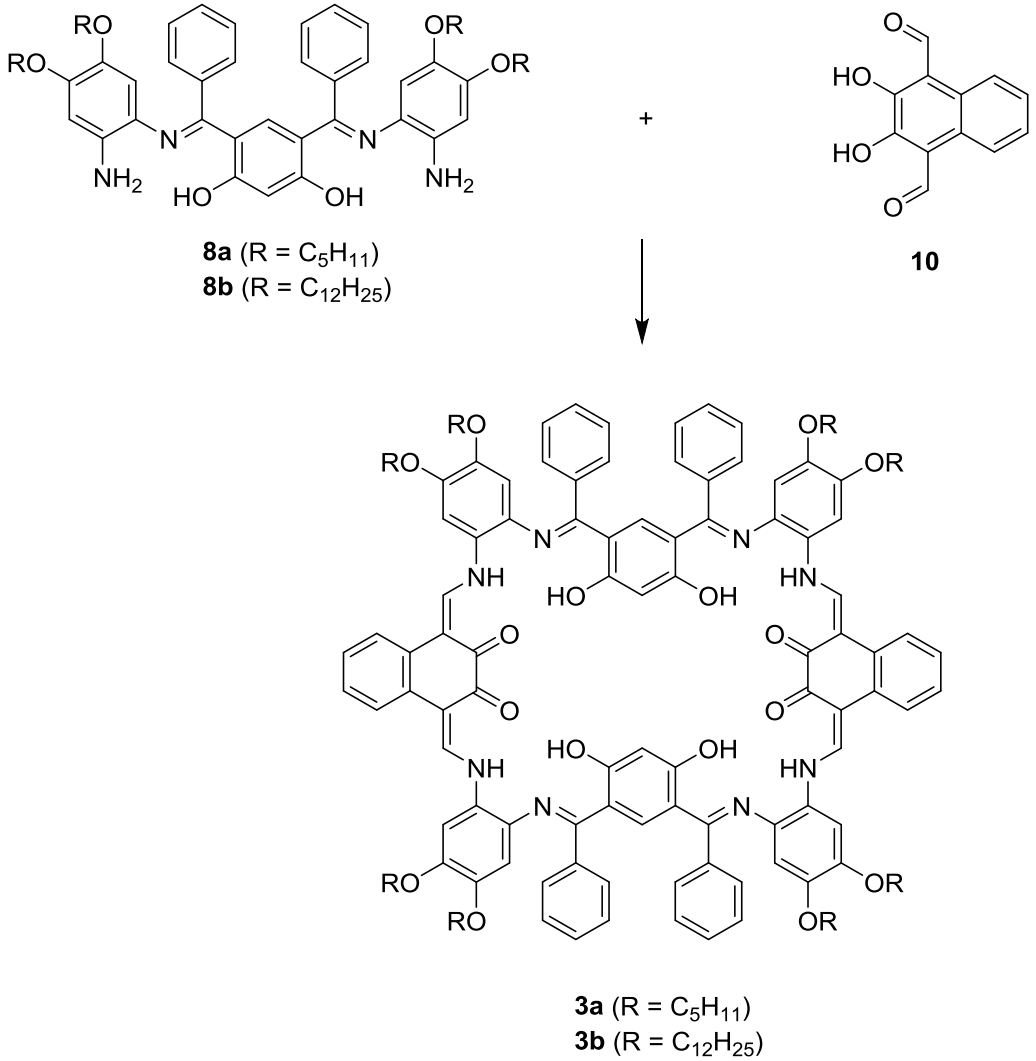

Synthesis of 3a. Compound **8a**[2] (0.186 g, 0.22 mmol) and compound **10**[4] (0.047 g, 0.22 mmol) were dissolved in a mixture of 120 mL of dry, degassed chloroform and 40 mL of dry, degassed acetonitrile. After the red solution was stirred at room temperature for 5 min, piperidine (0.04 mL, 0.41 mmol) was added, resulting in a

darkening of the solution. The resulting mixture was heated at reflux under nitrogen overnight. After cooling to room temperature, solvent was evaporated by rotary evaporation. Addition of methanol yielded a red precipitate that was isolated by filtration. Recrystallization from chloroform/methanol afforded pure **3a** (0.078 g, 0.038 mmol) in 35% yield.

Data for 3a. ^{1}H NMR ($CDCl_3$, 320 K) : δ 14.85 (s, 4H), 14.67 (d, 4H), 8.76 (d, 4H), 7.69 (m, 4H), 7.19-6.88 (m, 26H), 6.62 (s, 4H), 6.60 (s, 2H), 6.18 (s, 4H), 3.92 (t, 8H), 3.62 (t, 8H), 1.97-0.90 ppm (m, 88H); ^{13}C NMR (1,1,2,2-tetrachloroethane-d_2, 343 K): δ 174.4, 168.2, 152.3, 148.6, 147.9, 140.1, 135.0, 134.4, 133.5, 129.5, 128.9, 128.4, 128.3, 128.0, 127.1, 125.1, 120.2, 113.5, 111.5, 111.1, 107.3, 105.4, 99.9, 70.8, 70.2, 29.3, 29.0, 28.4, 28.3, 22.6, 22.5, 14.2 ppm; IR: υ = 3300, 3055, 2951, 2928, 2867, 1614, 1548, 1503, 1465, 1319, 1256, 1180, 1124, 984, 915, 846, 740, 698, 555, 462 cm^{-1}; UV-vis (CH_2Cl_2) : λ_{max} (ε) = 479 (5.91×10^4), 382 (6.99×10^4), 289 (1.13×10^5) nm (L mol^{-1} cm^{-1}); Anal. Calcd for $C_{128}H_{141}N_8O_{16}\cdot3H_2O$: C 73.15; H 7.05; N 5.33. Found: C 73.30; H 6.50; N 5.22. MALDI-TOF MS: m/z 2047.1 $[M+H]^+$; HRMS (ESI): $C_{128}H_{141}N_8O_{16}$ Calcd: 2046.0466, Found: 2046.0508. mp = dec. at 280 °C.

Synthesis of macrocycle 3b. Compound **8b**[5] (0.20 g, 0.16 mmol) and compound **10**[4] (0.035 g, 0.16 mmol) were dissolved in a mixture of 120 mL of dry, degassed chloroform and 50 mL of dry, degassed acetonitrile. After the red solution was stirred at room temperature for 5 min, piperidine (0.04 mL, 0.41 mmol) was added, resulting in a darkening of the solution. The resulting mixture was heated at reflux under nitrogen overnight. After cooling to room temperature, solvent was evaporated by rotary evaporation. Addition of ethanol yielded a red precipitate that was isolated by filtration. Recrystallization from chloroform/methanol and filtering afforded 0.086 g of asphalt-like macrocycle **3b** (0.033 mmol, 41%).

Data for 3b. ^{1}H NMR (400 MHz, $CDCl_3$, 298 K) : δ 14.95 (s, 4H), 14.78 (d, 4H), 8.73 (d, 4H), 7.68 (m, 4H), 7.19 (m,4H), 7.06-6.89 (m, 22H), 6.60 (s, 4H), 6.59 (s, 2H), 3.91 (t, 8H), 3.58 (t, 8H), 1.76-0.83 (m, 184H) ppm. ^{13}C NMR (150.6 MHz, $CDCl_3$, 298 K, 48 h): 173.3, 167.4, 151.4, 147.0, 146.6, 139.0, 133.7, 132.1, 128.1, 127.8, 127.5, 126.3, 124.2, 119.3, 112.6, 110.5, 109.1, 105.0, 104.8, 69.4, 68.7, 31.5, 29.3, 29.2, 29.0, 28.9, 28.4, 25.6, 25.4, 22.3, 13.7 ppm. IR: υ = 3300, 3050, 2948, 2930, 1618, 1550, 1503, 1447, 1320, 1250, 1181, 982, 850, 741, 699, 554, 422 cm^{-1}. UV-Vis ($CHCl_3$, 1 cm cuvette, c = 6.8×10^{-5} M): λ_{max} (ε) = 480 (5.62×10^4), 382 (6.68×10^4), 286 (1.09×10^5) nm (L mol^{-1} cm^{-1}); Anal. Calcd for $C_{184}H_{252}N_8O_{16}\cdot3H_2O$: C 76.57; N 3.88; H 9.01. Found: C 76.53; N 3.83; H 8.89. MALDI-TOF MS (dithranol matrix): *m/z* 2831.9 $[M]^{\cdot+}$, 2854.9 $[M+Na]^+$, 2870.0 $[M+K]^+$; mp = 232-235 ^{o}C.

Table S1. Binding constant (K) of the complexes formed by association of macrocycles and guests[a]

	guest $\mathbf{4}^+$	guest $\mathbf{5}^+$	guest $\mathbf{6}^+$
	K (M^{-1})	K (M^{-1})	K (M^{-1})
Macrocycle **1a**	$1.85\pm0.37\times10^4$ *b*	$2.12\pm0.48\times10^4$	$3.24\pm0.41\times10^3$ *b*
Macrocycle **3a**	$4.67\pm0.71\times10^4$	$4.34\pm0.65\times10^4$	$2.54\pm0.53\times10^3$

[a] Measured at 300 K in $CDCl_3$. The concentration of hosts was kept constant at 6.11×10^{-4} M during titration. Binding constants were obtained using the curve fitting program Sigmaplot 10 and EQNMR (M. J. Hynes, *J. Chem. Soc., Dalton Trans.*, 1993, 311). Both methods gave essentially the same result. [b] Data from reference 9 of the paper (J. Jiang and M. J. MacLachlan, *Chem. Commun.*, 2009, 5695).

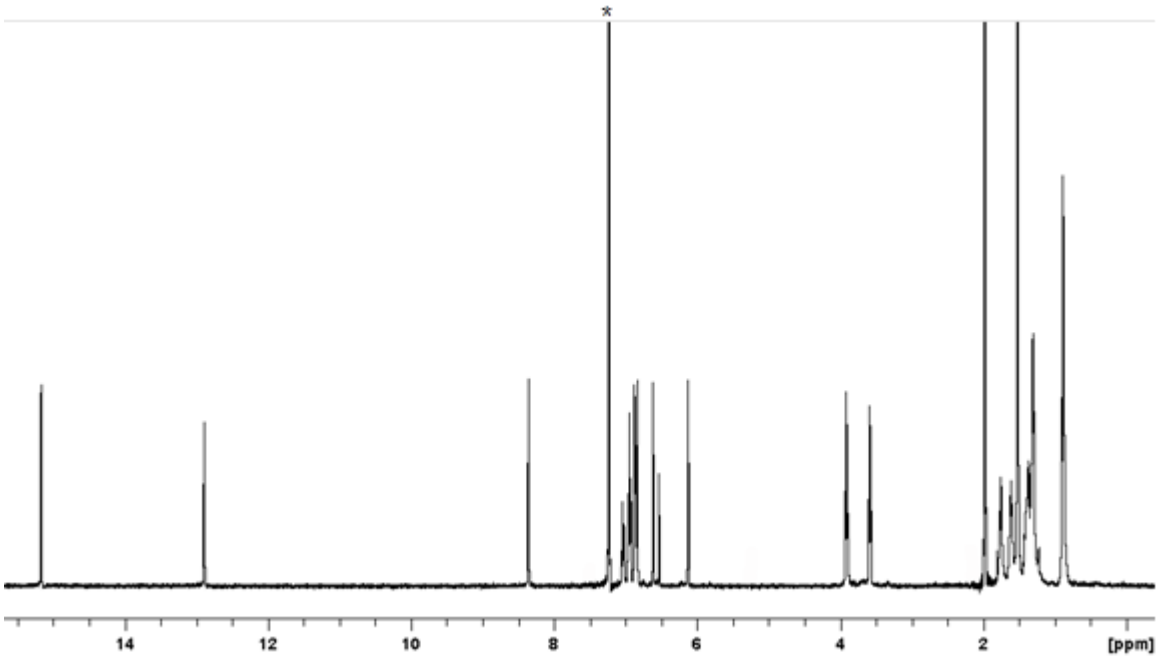

Figure S1. ^{1}H NMR spectrum of macrocycle **1b** ($CDCl_3$, 400 MHz, 298 K) (* = $CHCl_3$)

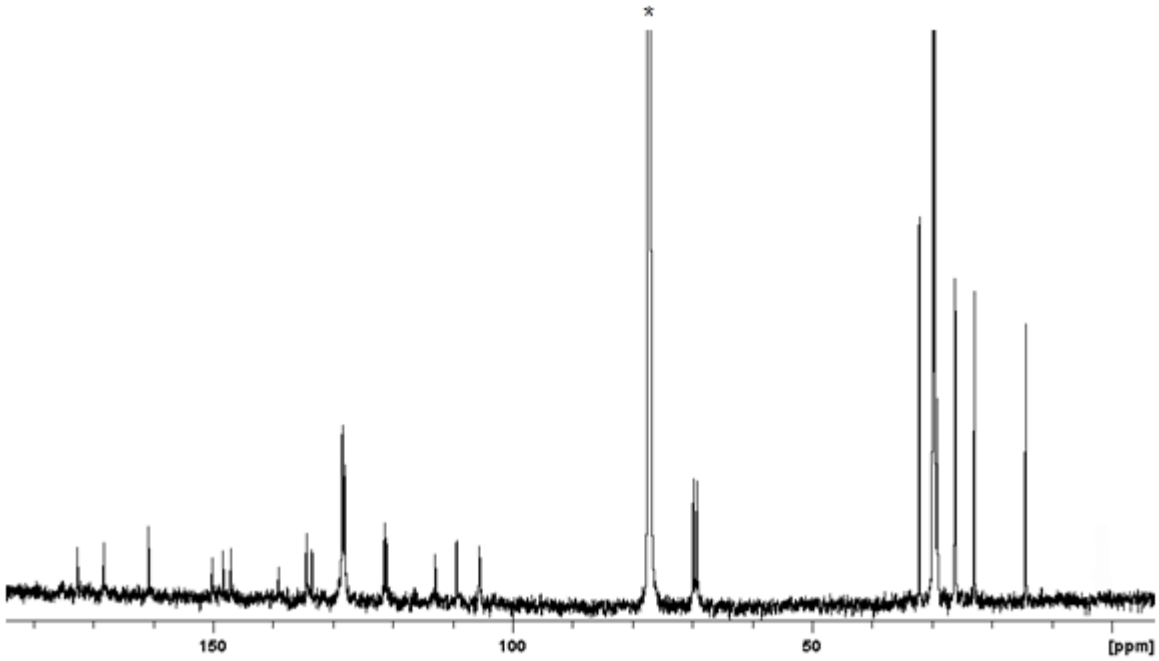

Figure S2. ^{13}C NMR spectrum of macrocycle **1b** ($CDCl_3$, 400 MHz, 298 K) (* = $CDCl_3$)

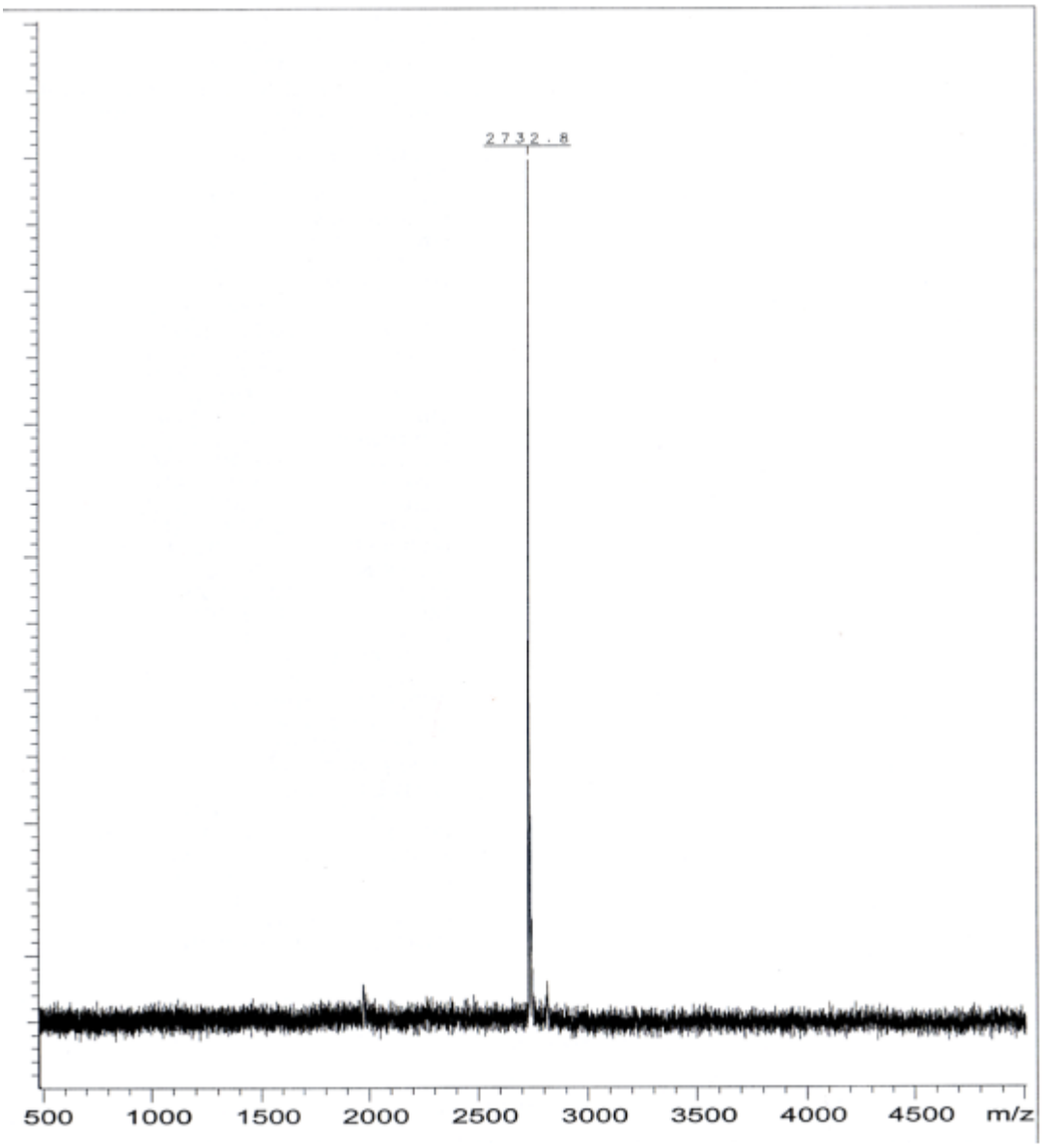

Figure S3. MALDI-TOF mass spectrum of compound **1b**

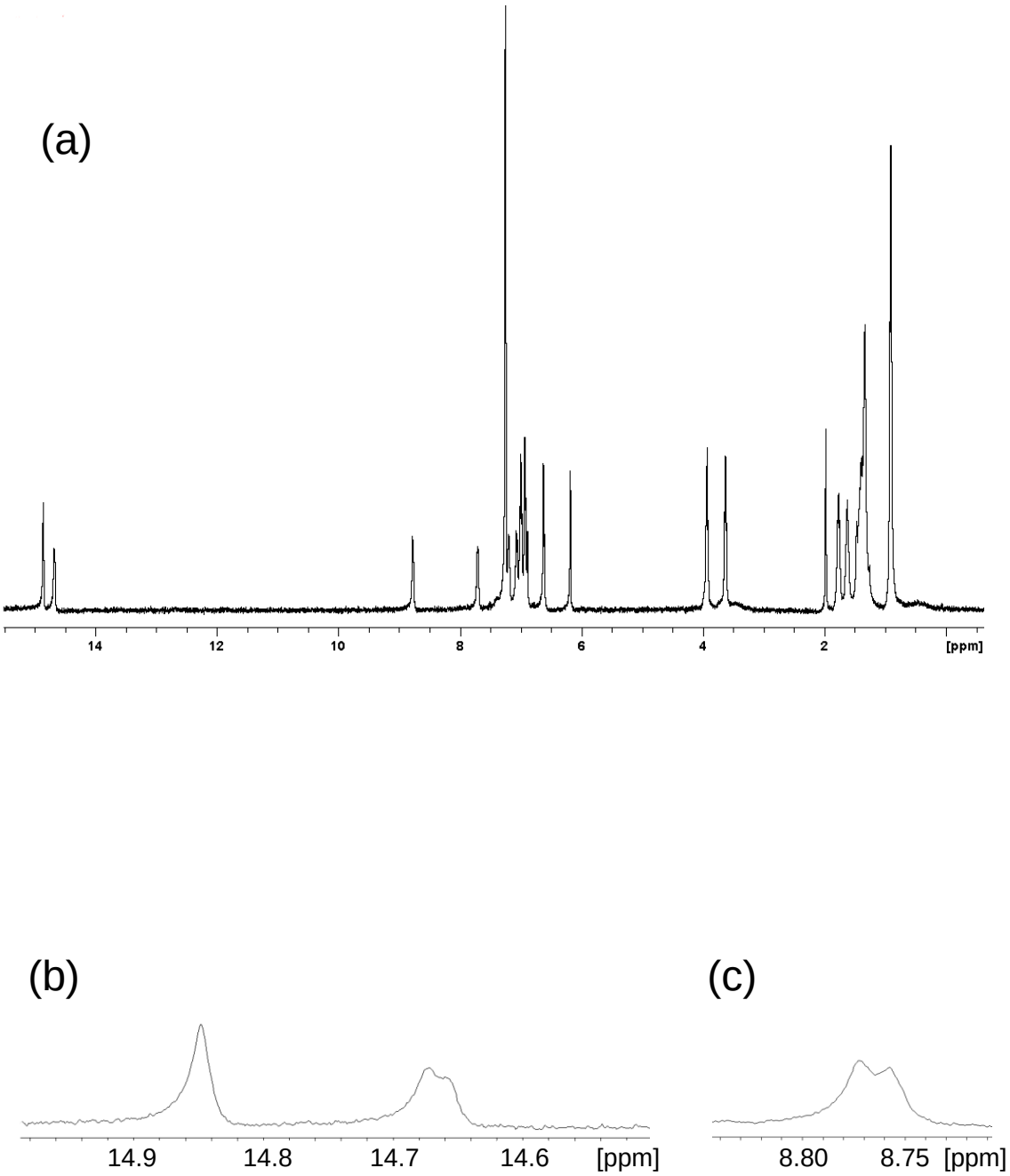

Figure S4. (a) ^{1}H NMR spectrum of macrocycle **3a**. ($CDCl_3$, 400 MHz, 320 K) (b) Enlarged ^{1}H NMR spectrum from 14.6 - 14.9 ppm. (c) Enlarged ^{1}H NMR spectrum from 8.75 - 8.80 ppm.

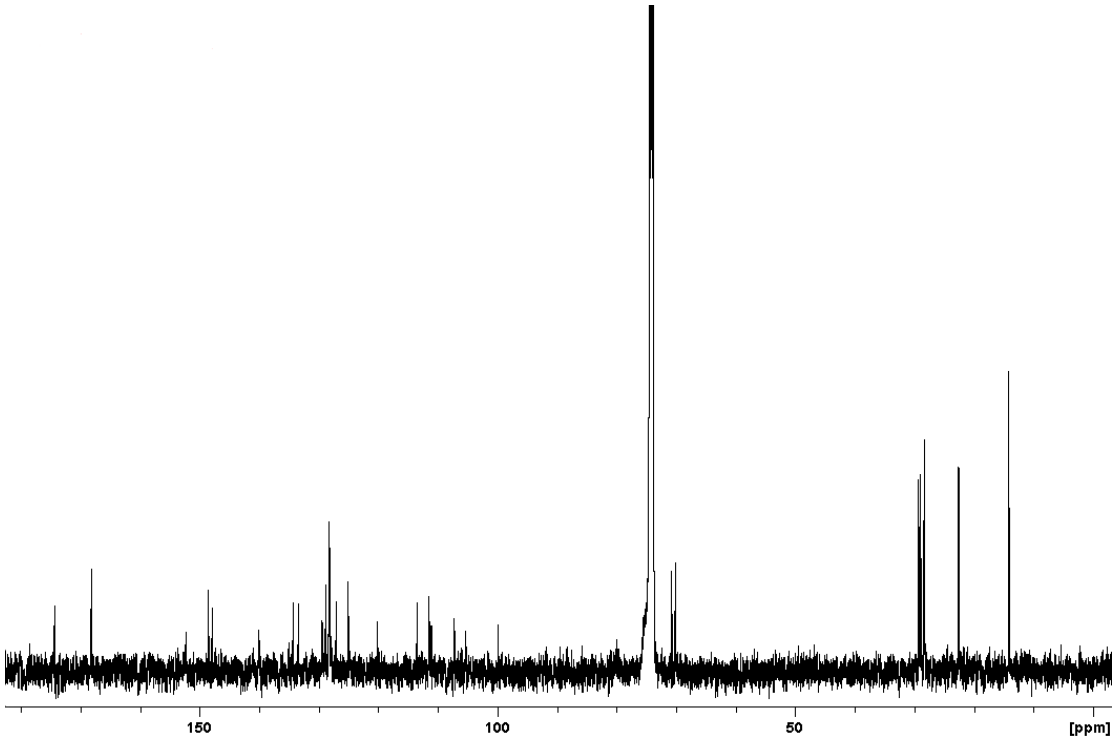

Figure S5. ^{13}C NMR spectrum of macrocycle **3a** (1,1,2,2-tetrachloroethane-d_2, 343K)

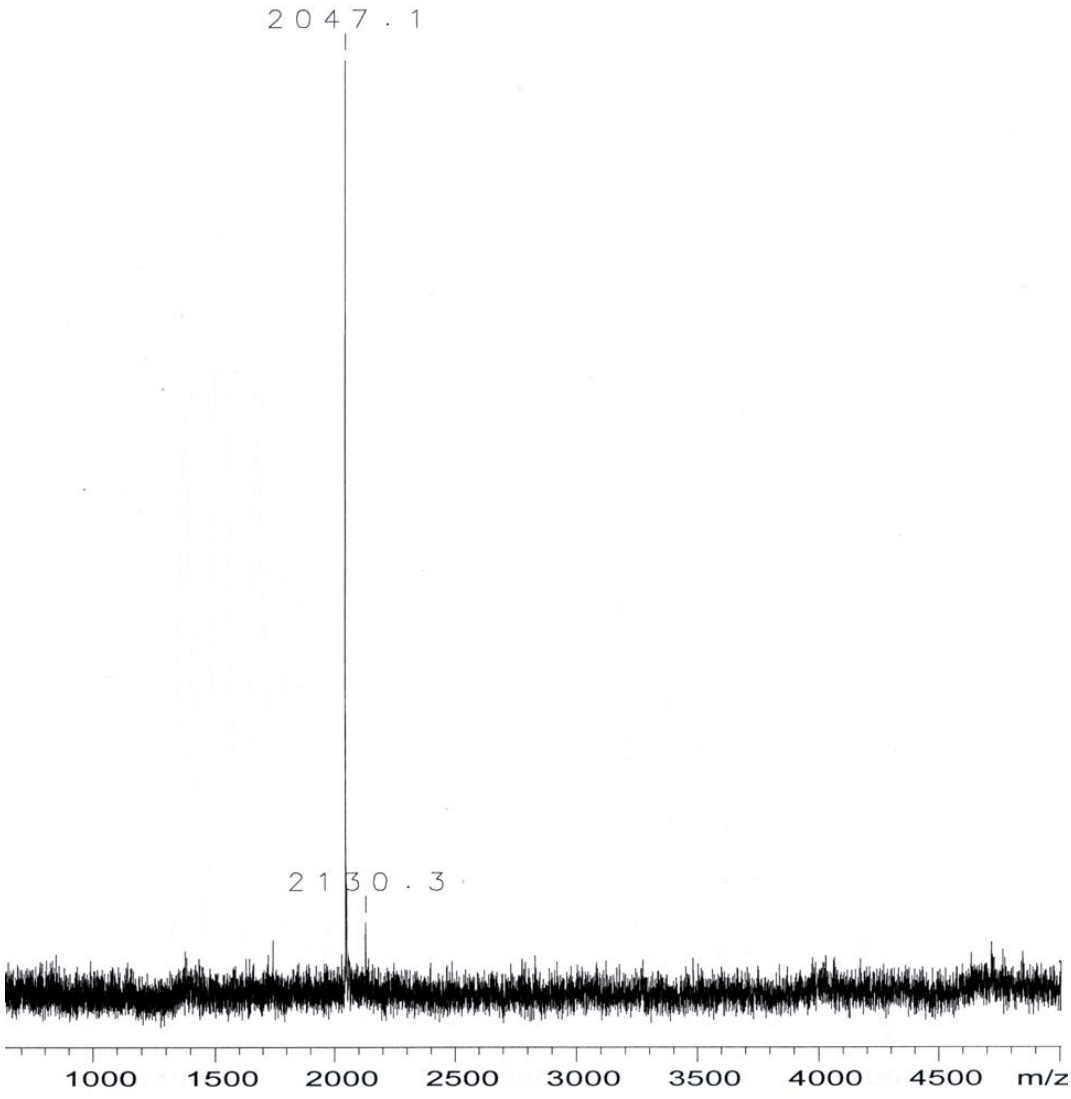

Figure S6. MALDI-TOF mass spectrum of macrocycle **3a**

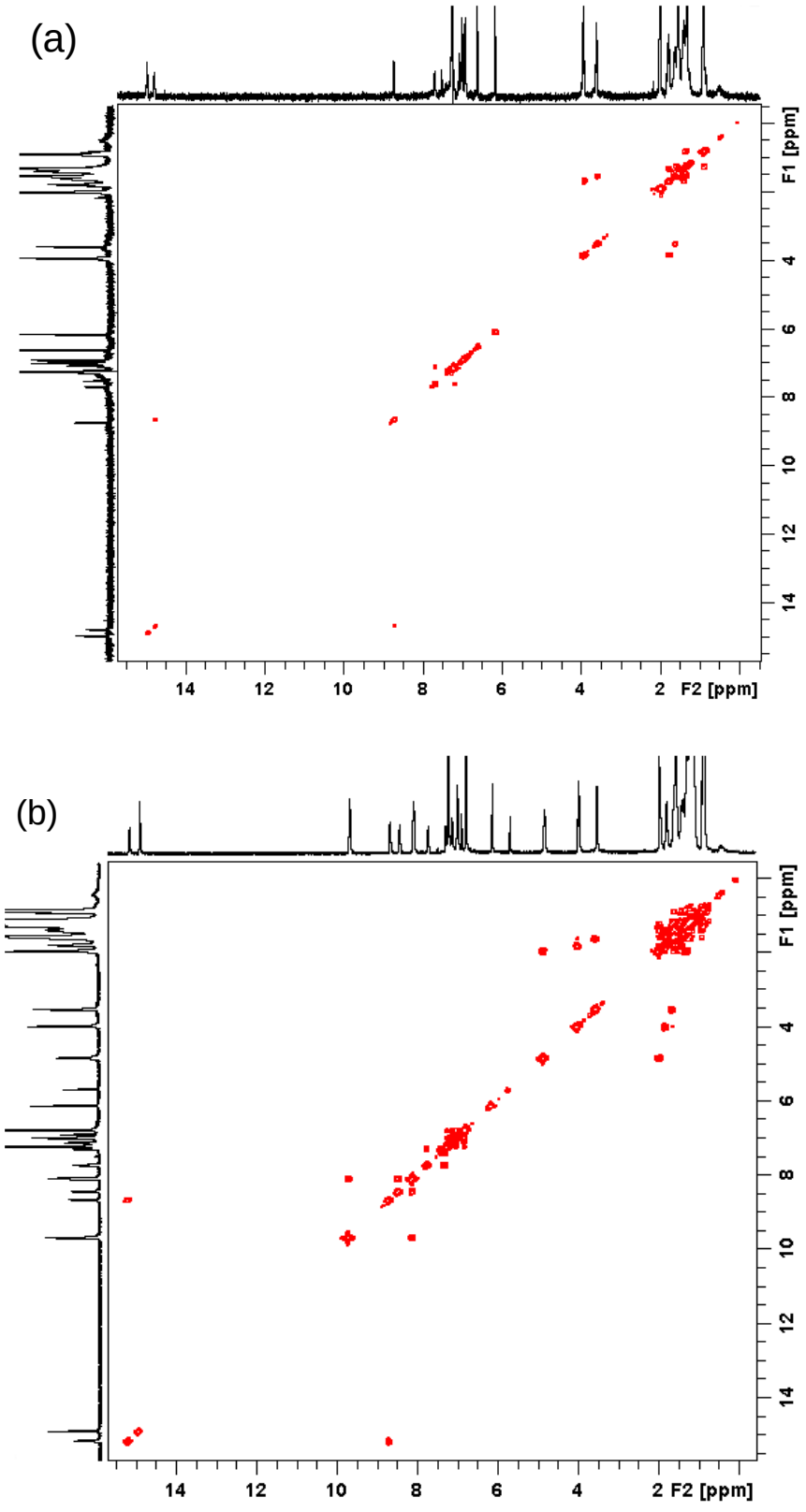

Figure S7. (a) ^{1}H-^{1}H COSY NMR spectrum of macrocycle **3a**. (b) ^{1}H-^{1}H COSY NMR spectrum of complex formed by macrocycle **3a** and cetylpyridinium chloride **4**$^{+}$·Cl^{-}(the ratio of **3a** and **4**$^{+}$·Cl^{-} used was 1:5)

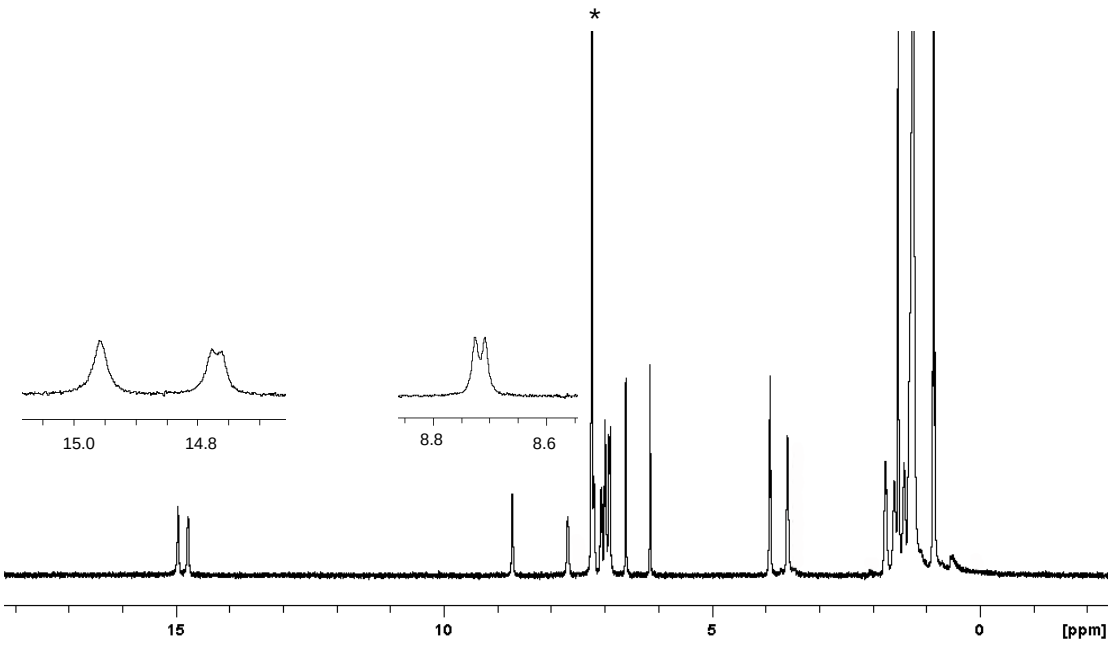

Figure S8. ^{1}H NMR spectrum of macrocycle **3b** ($CDCl_3$, 400 MHz, 298 K, c = 2.6 × 10^{-4} M) (* = $CHCl_3$)

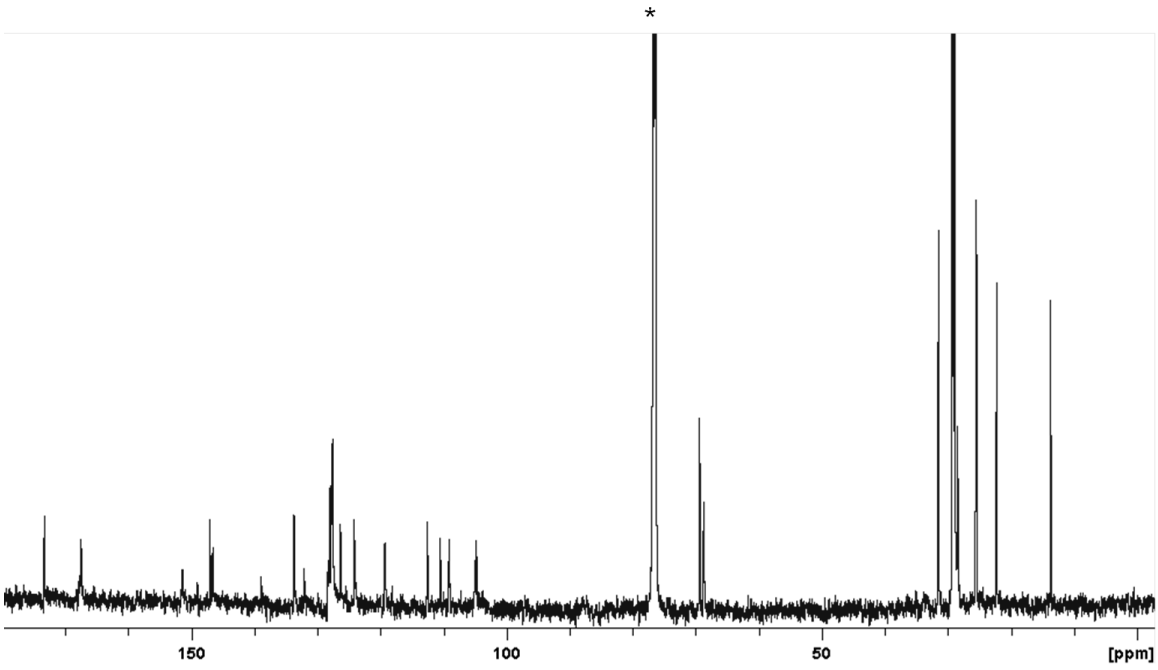

Figure S9. ^{13}C NMR spectrum of macrocycle **3b** ($CDCl_3$, 150 MHz, 298 K, c = 2.6 × 10^{-4} M, 48 h) (* = $CDCl_3$)

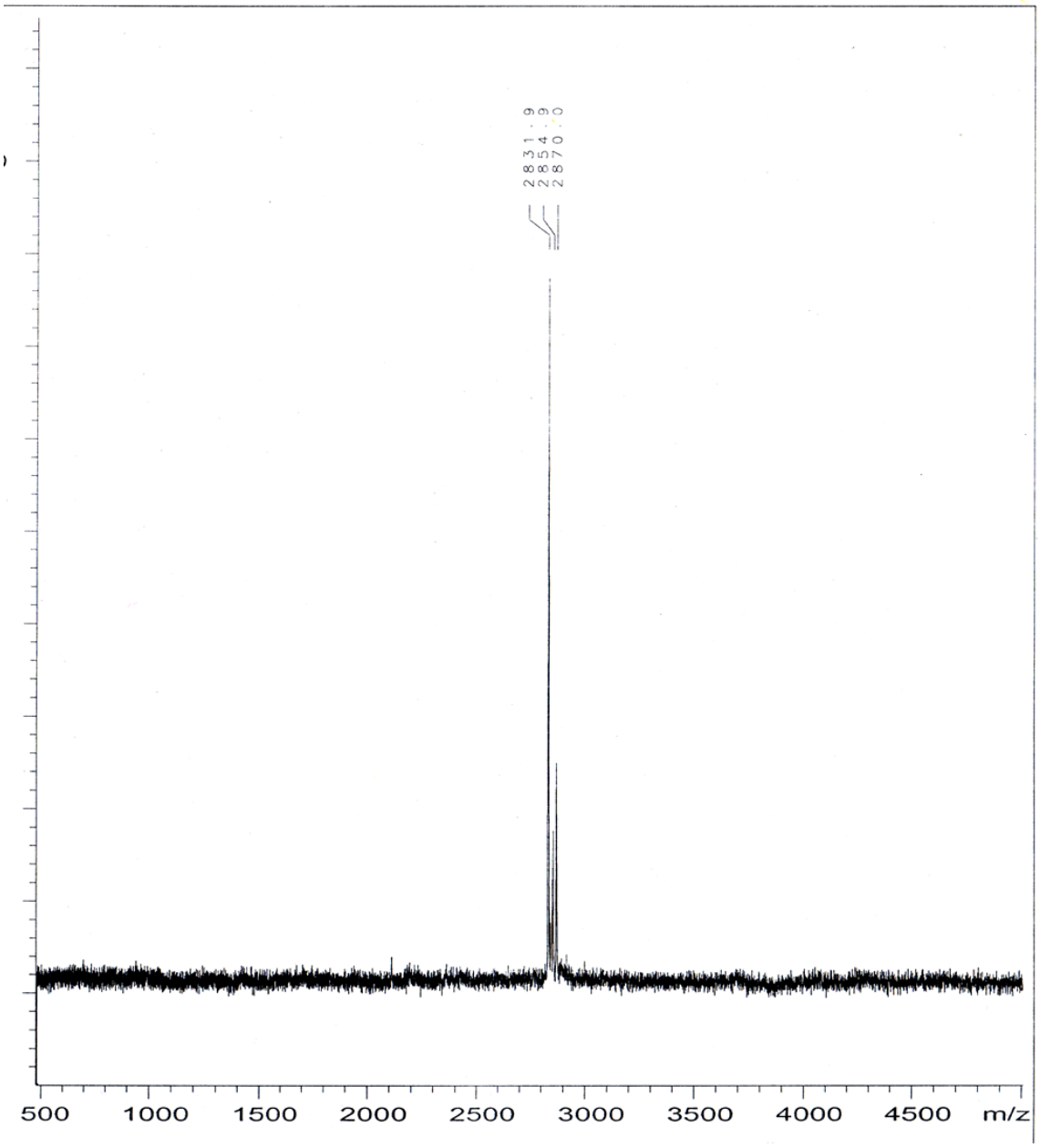

Figure S10. MALDI-TOF mass spectrum of macrocycle **3b**. The peaks are at *m/z* 2831.9 $[M]^{\cdot+}$, 2854.9 $[M+Na]^{+}$, and 2870.0 $[M+K]^{+}$.

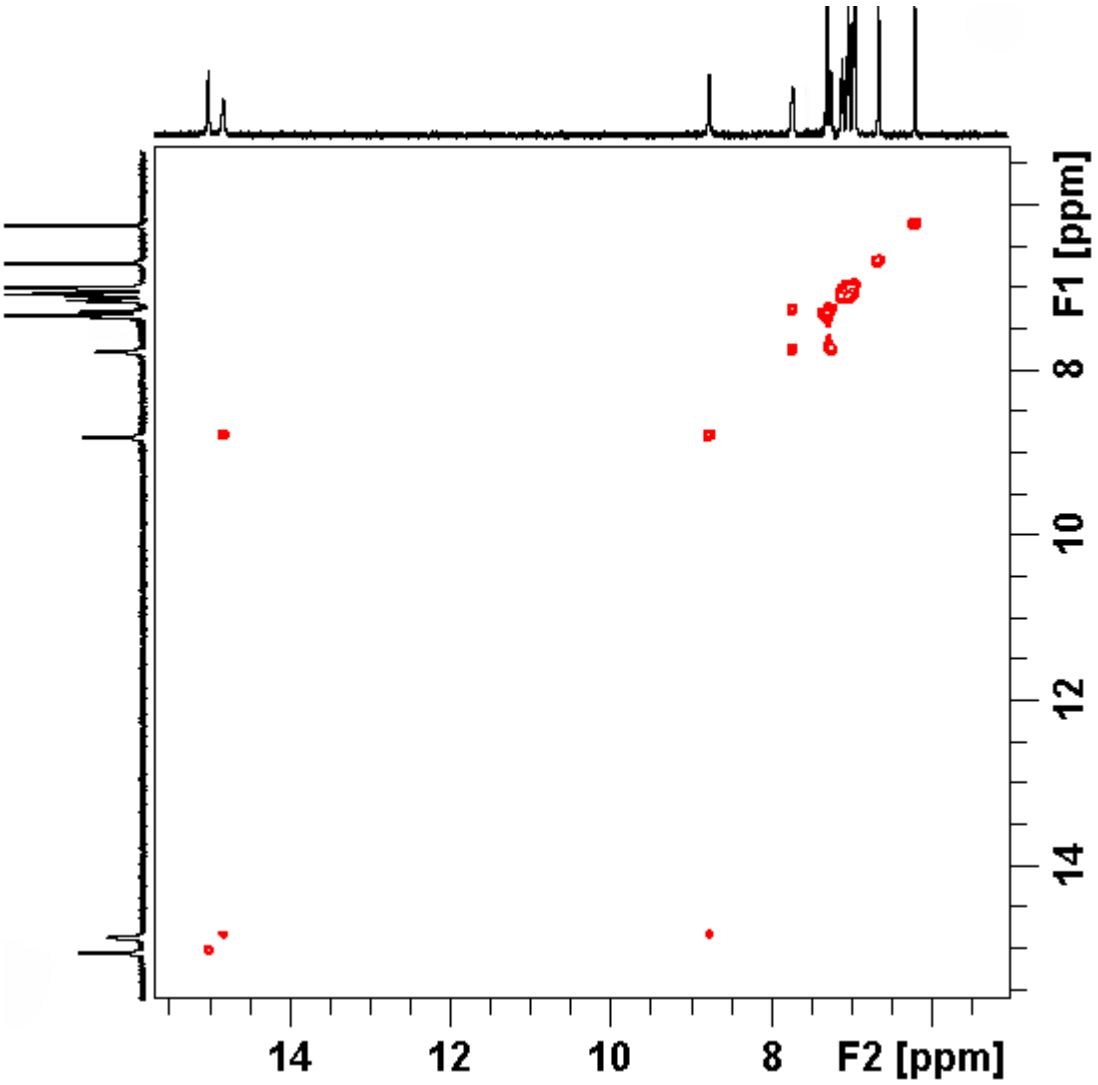

Figure S11. Partial of 2D ^{1}H-^{1}H COSY NMR spectrum of macrocycle **3b** ($CDCl_3$, 400 MHz, 298 K, c = 2.6×10^{-4} M)

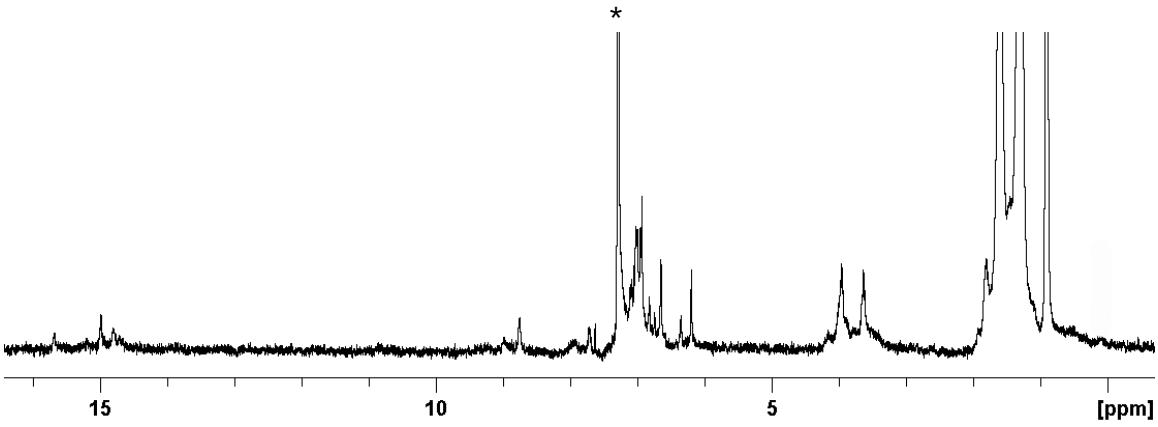

Figure S12. ^{1}H NMR spectrum of macrocycle **3b** at higher concentration ($CDCl_3$, 400 MHz, 298 K, c = 2.2×10^{-3} M) (* = $CHCl_3$)

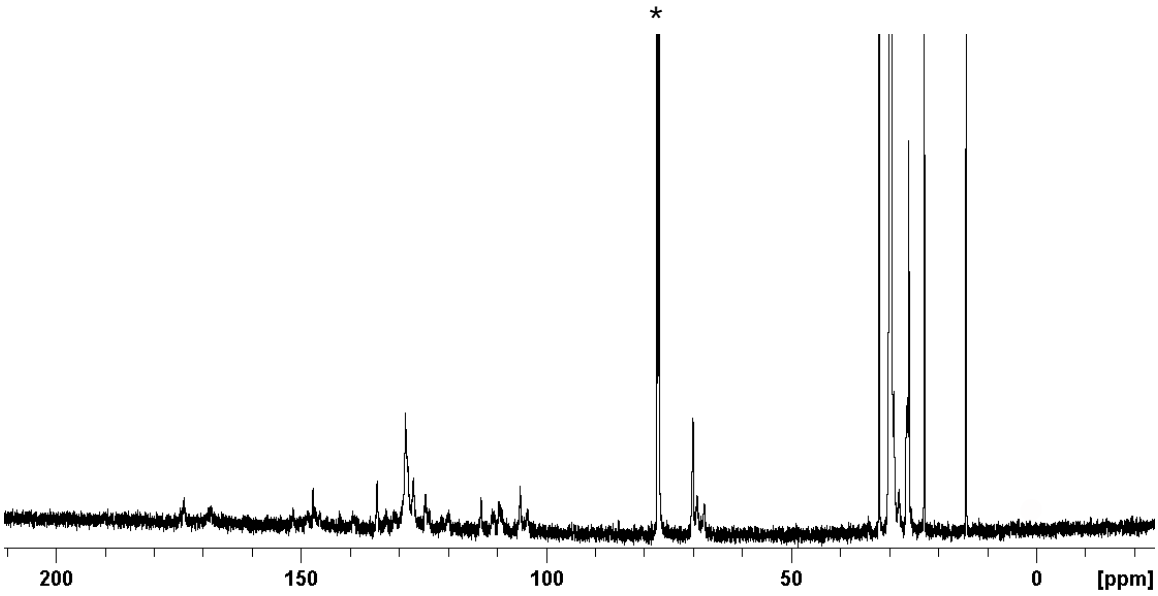

Figure S13. ^{13}C NMR spectrum of macrocycle **3b** at higher concentration ($CDCl_3$, 100 MHz, 298 K, c = 2.2×10^{-3} M) (* = $CDCl_3$)

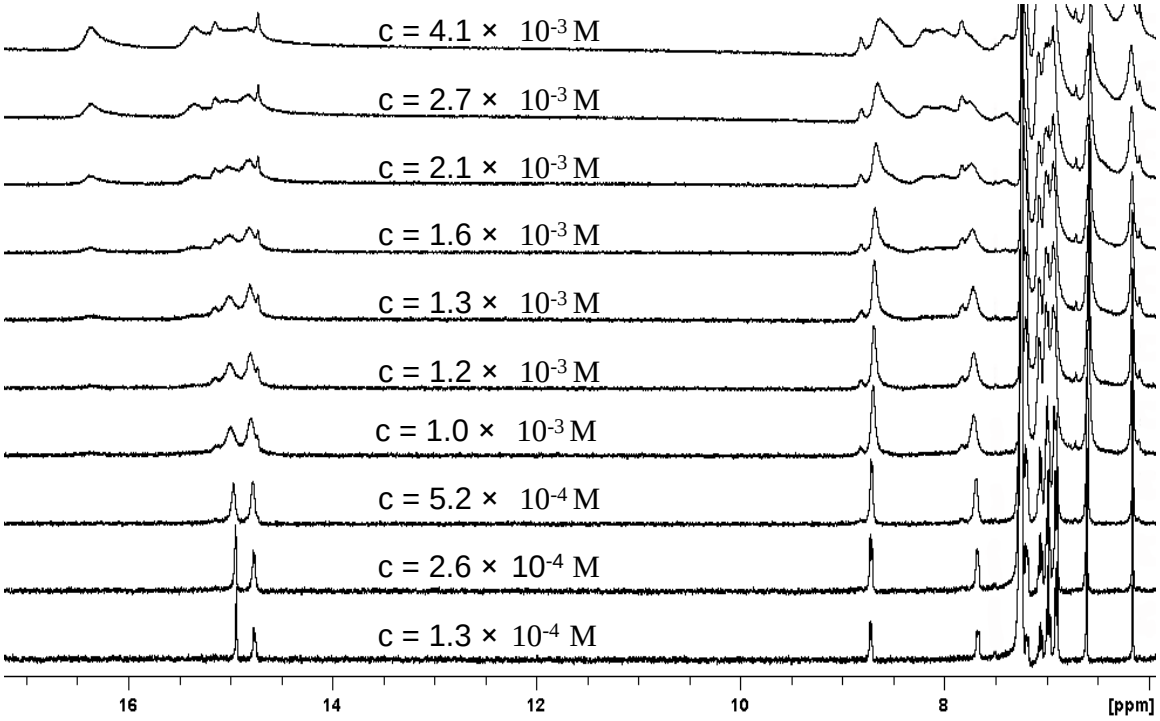

Figure S14. ^{1}H NMR spectra of macrocycle **3b** at different concentrations ($CDCl_3$, 400 MHz, 298 K)

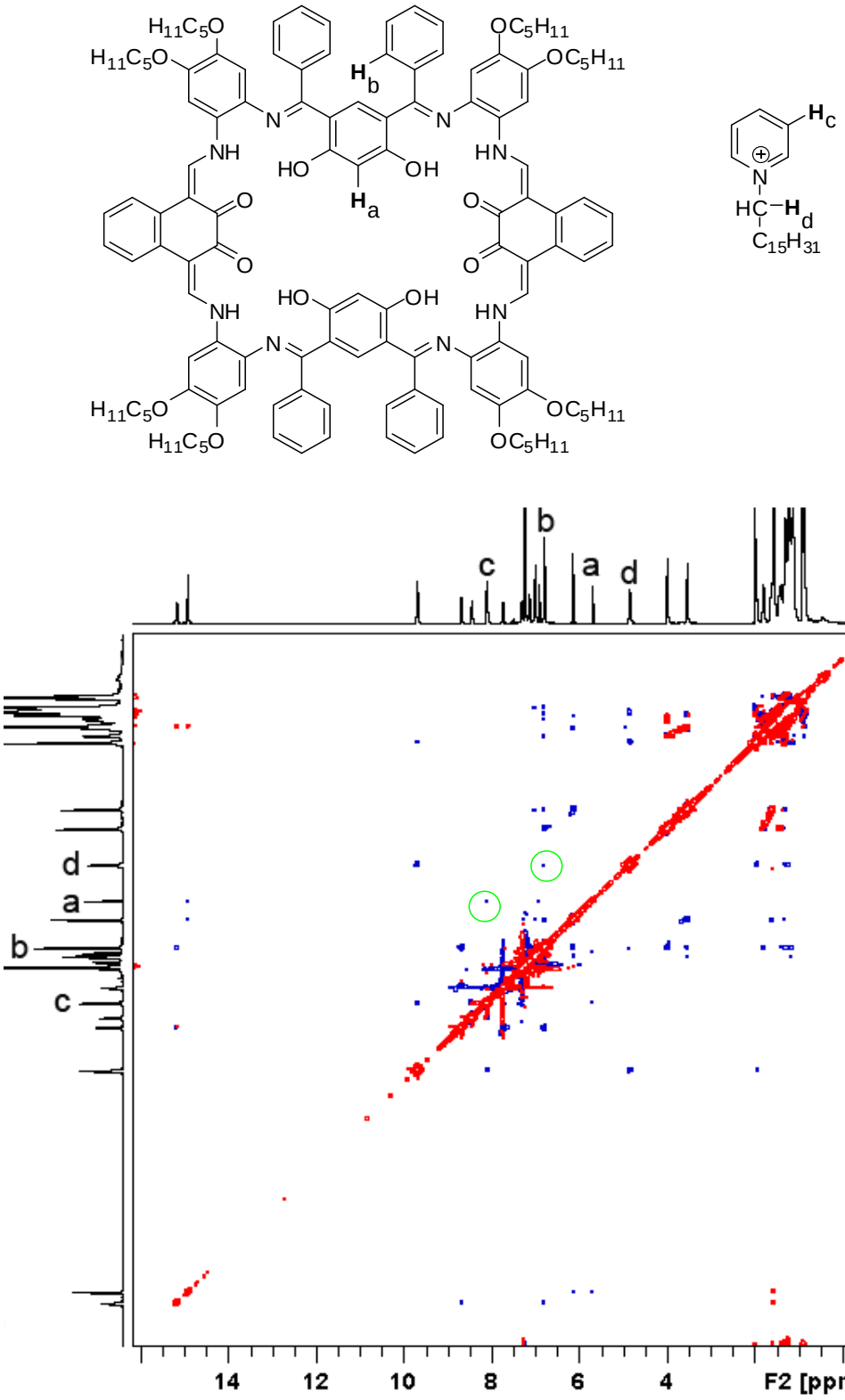

Figure S15. (a) 2D-ROESY NMR spectrum of complex formed by macrocycle **3a** and cetylpyridinium chloride $\mathbf{4}^{+}Cl^{-}$ with a mixing time of 120 ms (400 MHz, $CDCl_3$, 298 K). The circled crossings (H_a and H_c; H_b and H_d) are couplings between macrocycle **3a** and cetylpyridinium $\mathbf{4}^{+}$.

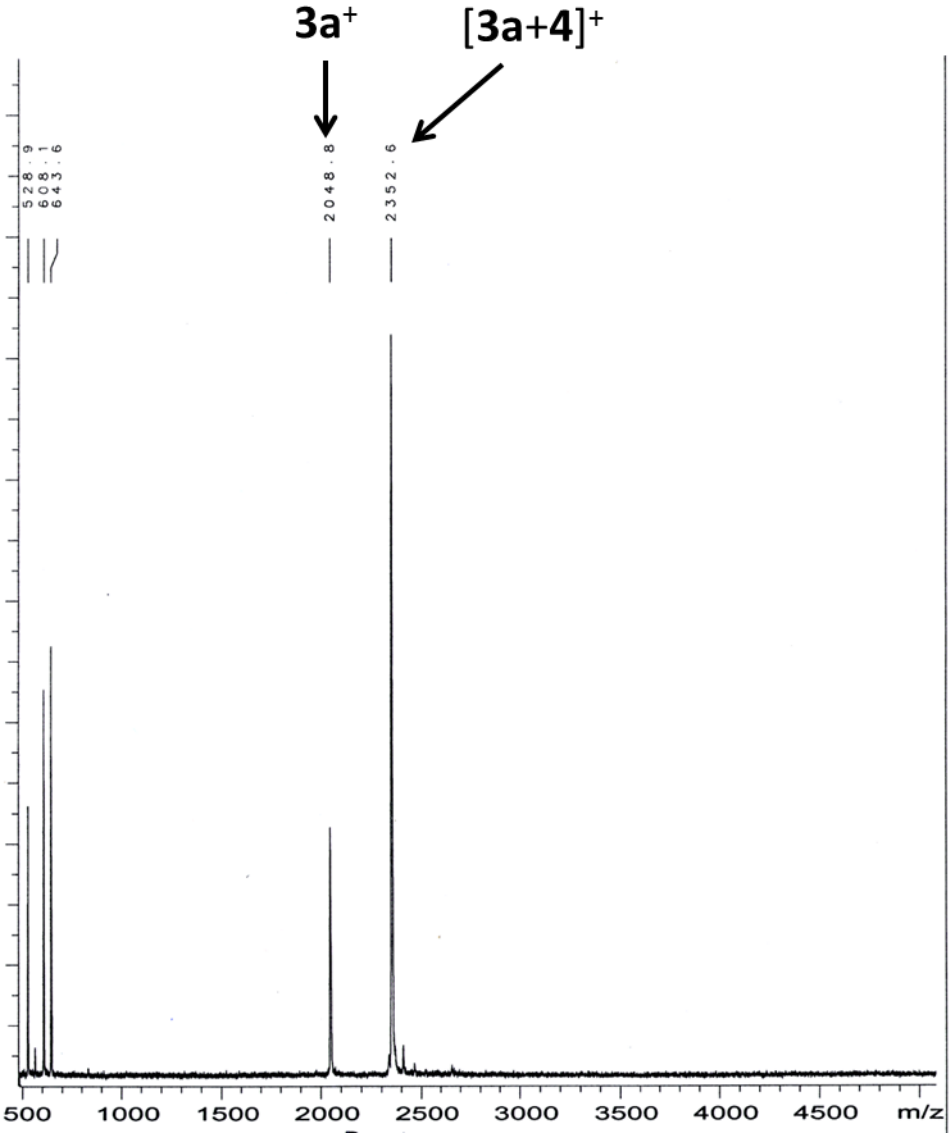

Figure S16. MALDI-TOF spectrum of complex between macrocycle **3a** and **4**$^{+}$·Cl^{-} cetylpyridinium chloride

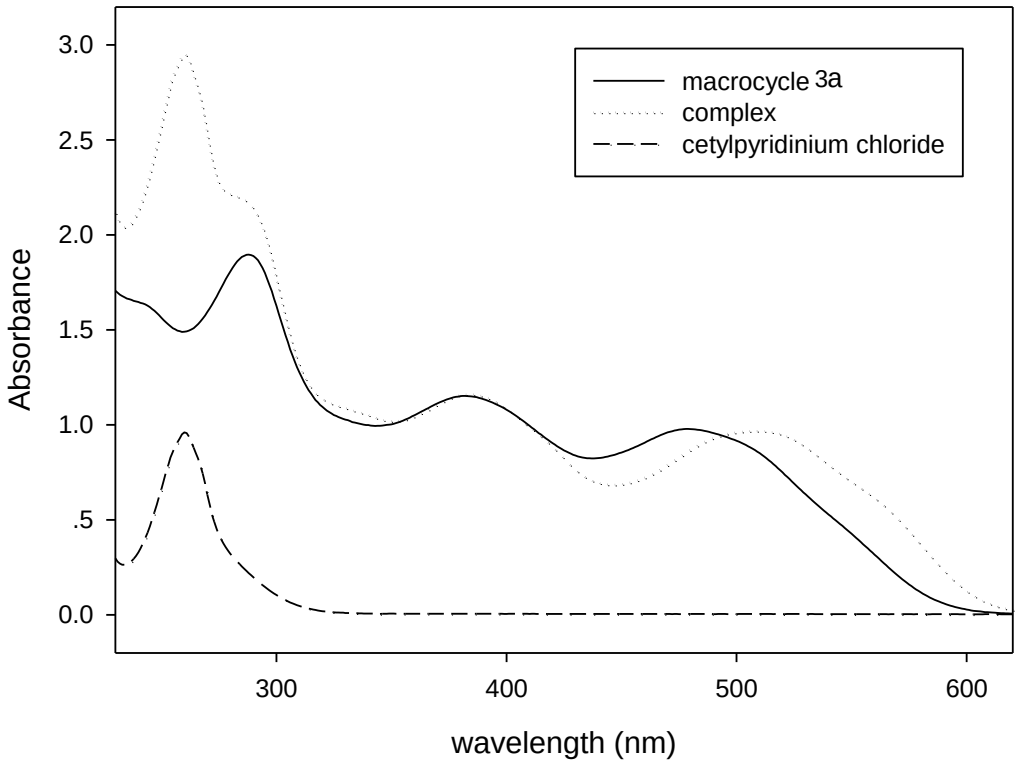

Figure S17. UV-vis spectrum (1.0 cm cell, 298 K, CH_2Cl_2) of 0.025 mM macrocycle **3a** (solid line), 0.141 mM cetylpyridinium chloride (dotted line) and mixture of 0.025 mM macrocycle **3a** and 0.141 mM cetylpyridinium chloride (dashed line)

(a)

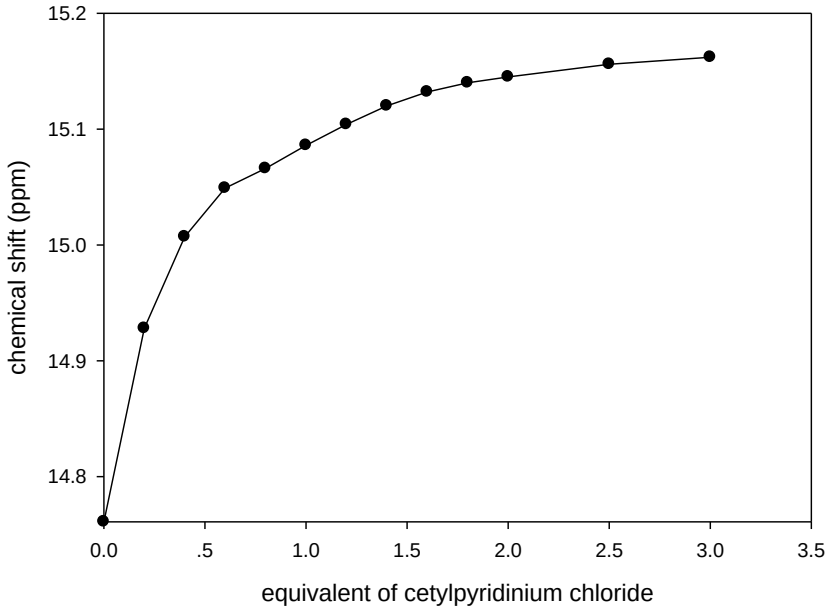

(b)

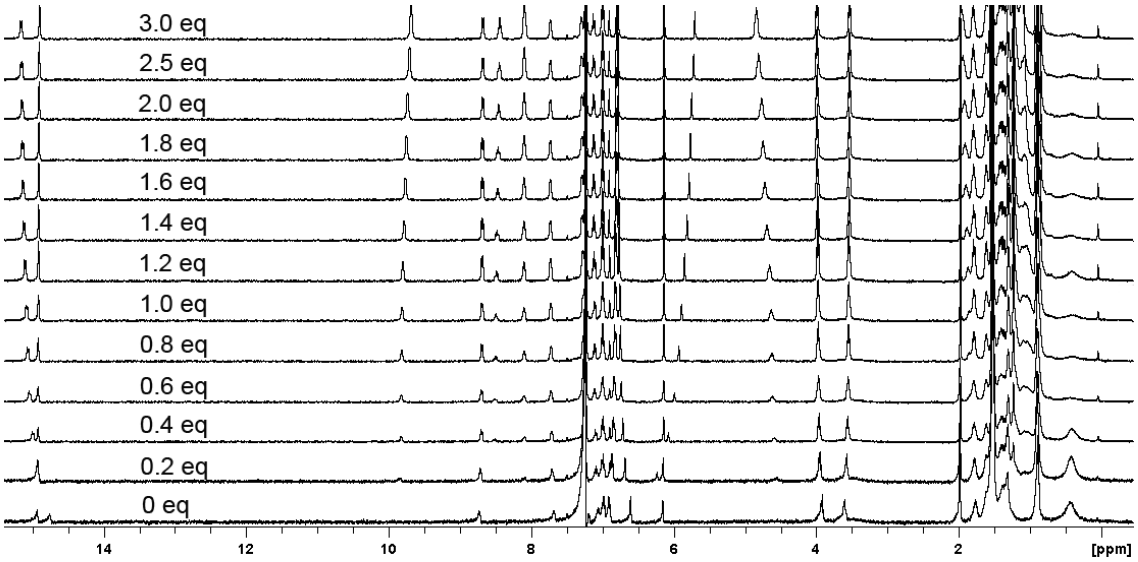

Figure S18. Titration curve (a) and stacked ^{1}H NMR spectra (b) of macrocycle **3a** with cetylpyridinium chloride $\mathbf{4}^{+}\cdot Cl^{-}$ (400 MHz, $CDCl_3$, 298 K)

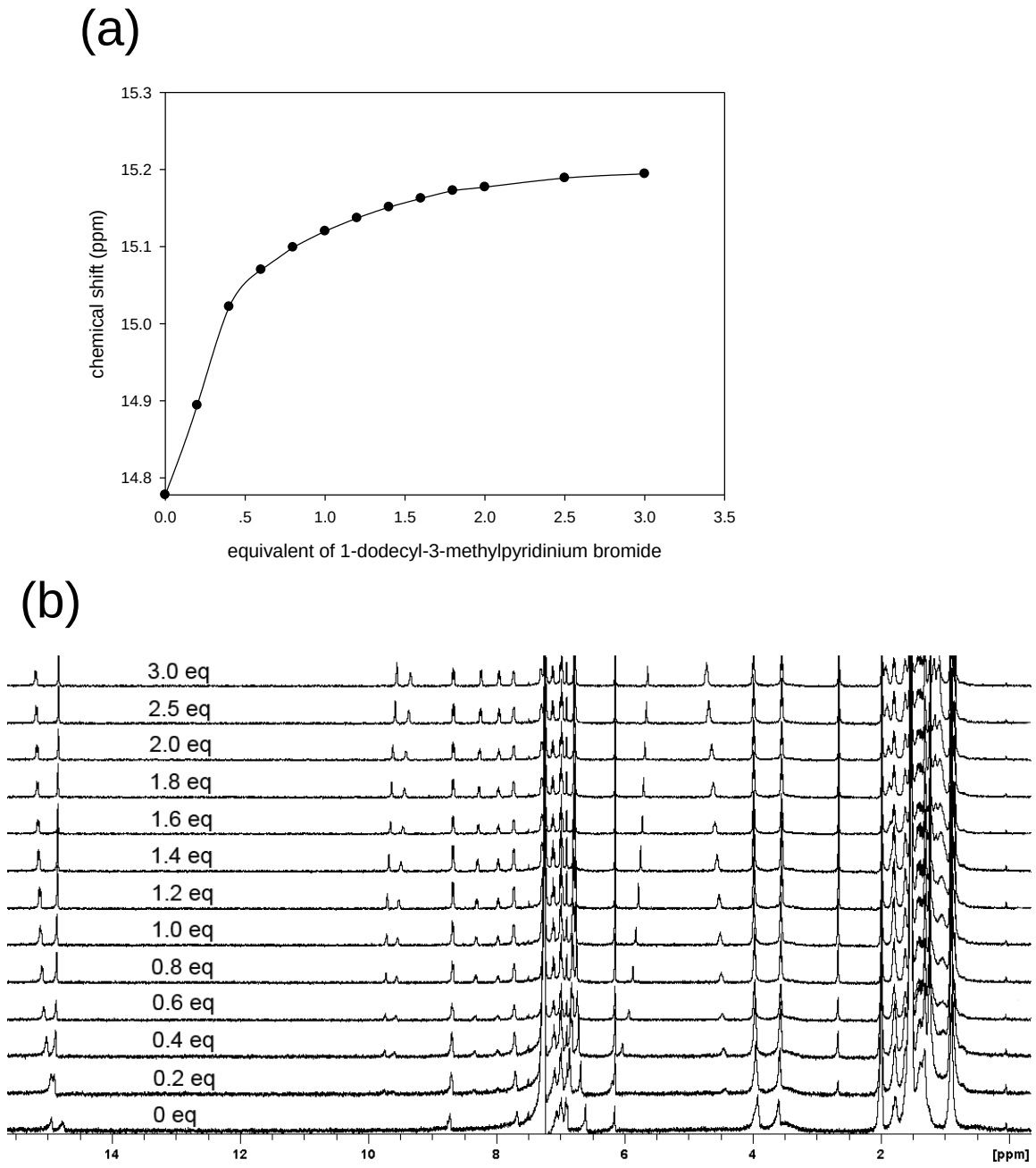

Figure S19. Titration curve (a) and stacked ^{1}H NMR spectra (b) of macrocycle **3a** with 1-dodecyl-3-methylpyridinium bromide $\mathbf{5}^{+}\cdot Br^{-}$ (400 MHz, $CDCl_3$, 298 K)

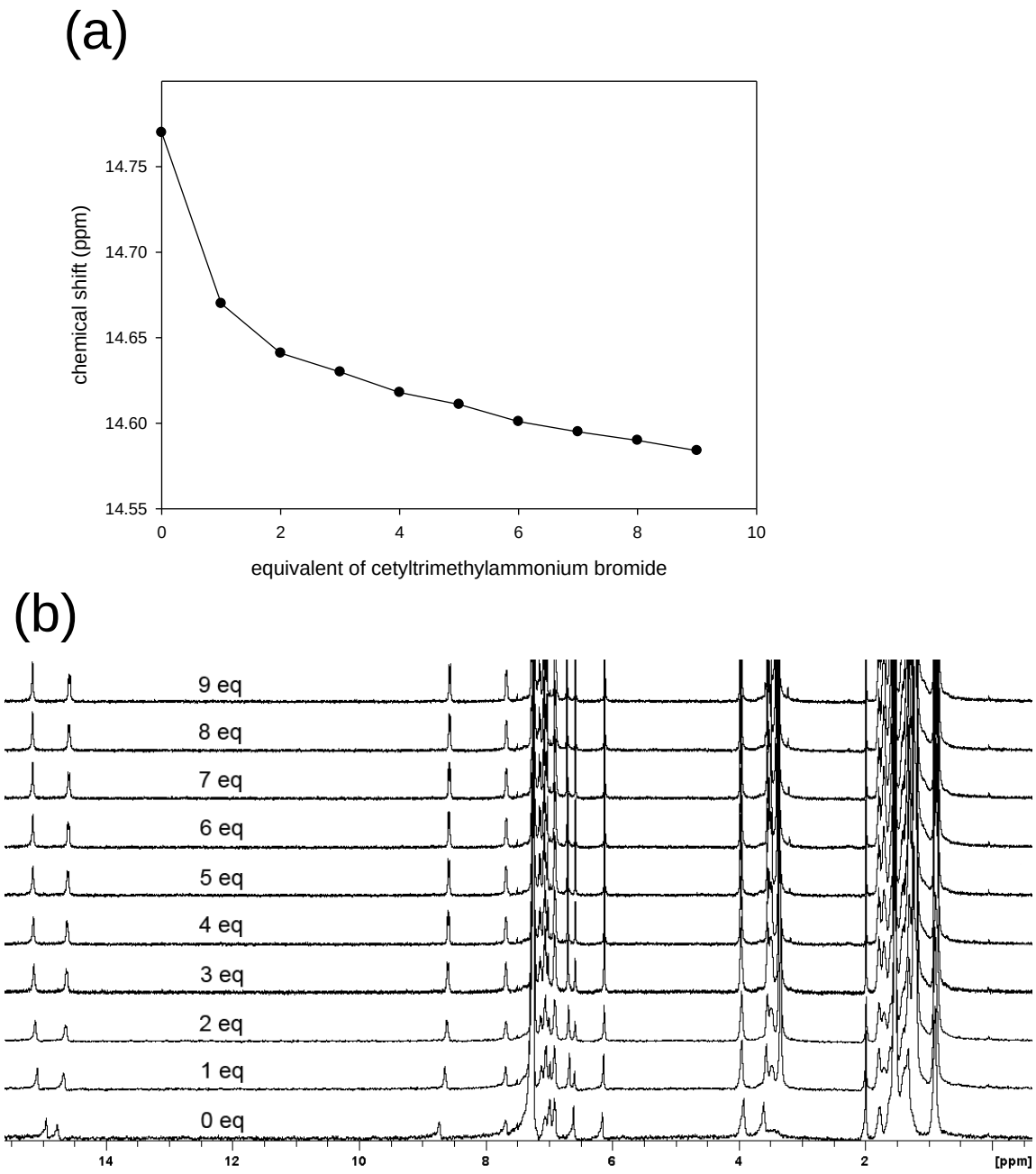

Figure S20. Titration curve (a) and stacked ^{1}H NMR spectra (b) of macrocycle **3a** with cetyltrimethylammonium bromide $\mathbf{6}^{+}\cdot Br^{-}$ (400 MHz, $CDCl_3$, 298 K)

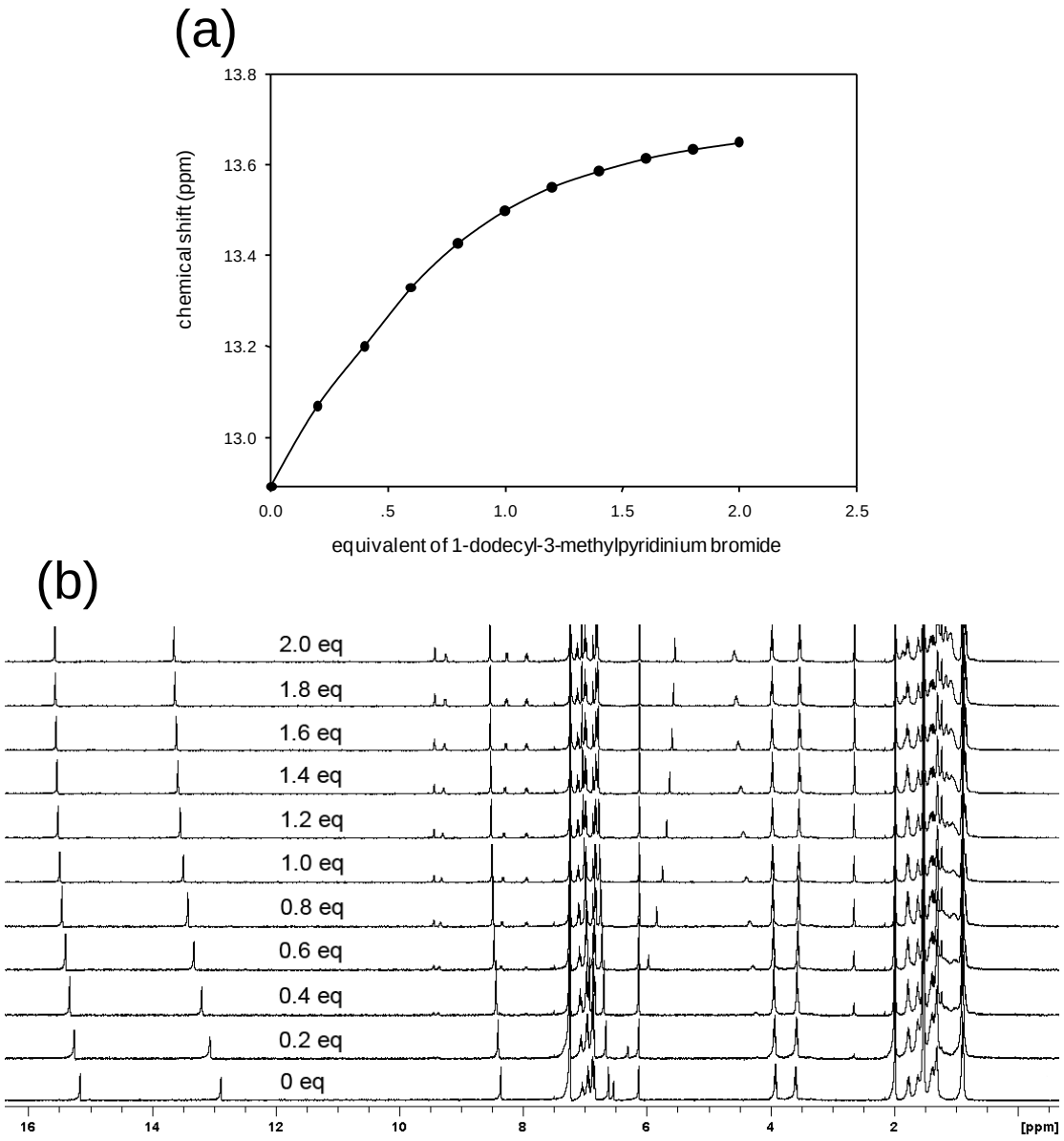

Figure S21. Titration curve (a) and stacked ^{1}H NMR spectra (b) of macrocycle **1a** with 1-dodecyl-3-methylpyridinium bromide $\mathbf{5}^{+}\cdot Br^{-}$ (400 MHz, $CDCl_3$, 298K)

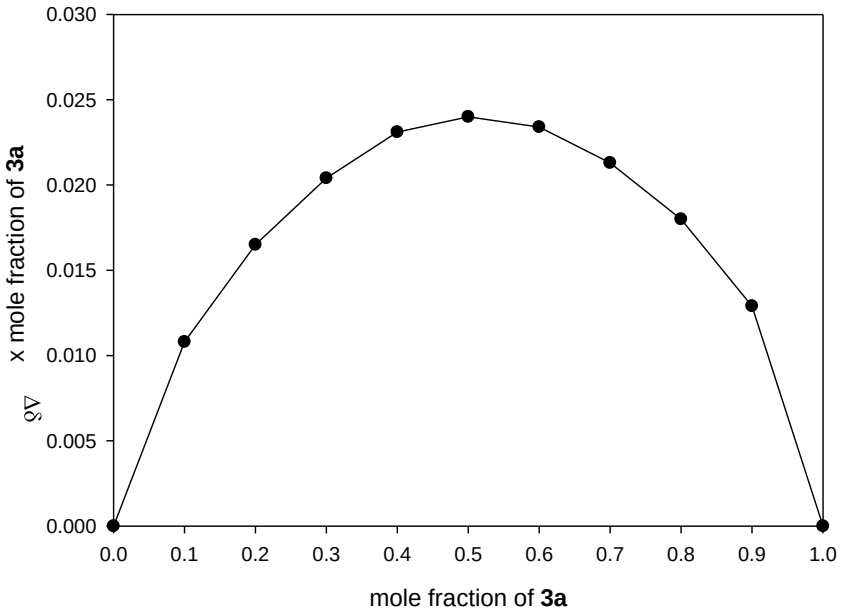

Figure S22. Job plot of macrocycle **3a** with cetylpyridinium chloride $\mathbf{4}^{+}\cdot Cl^{-}$ in $CDCl_3$.

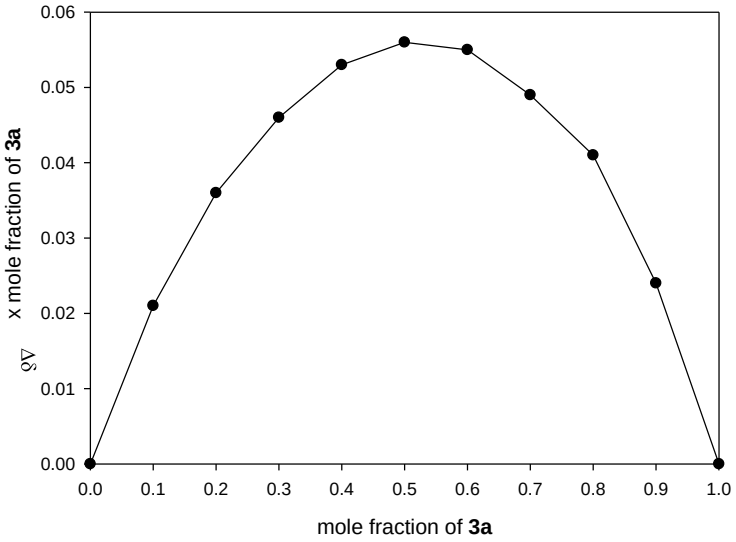

Figure S23. Job plot of macrocycle **3a** with 1-dodecyl-3-methyl-pyridinium bromide $\mathbf{5}^{+}\cdot Br^{-}$ in $CDCl_3$.

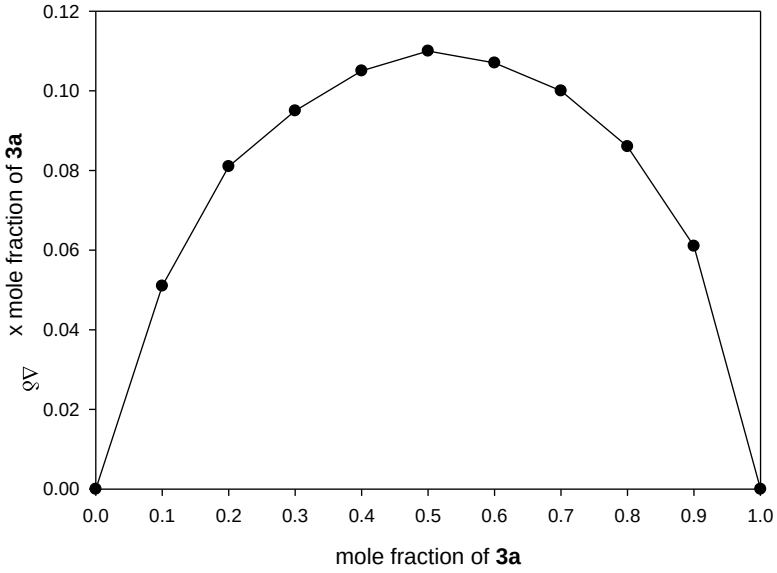

Figure S24. Job plot of macrocycle **3a** with cetyltrimethylammonium bromide $\mathbf{6}^{+}\cdot Br^{-}$ in $CDCl_3$.

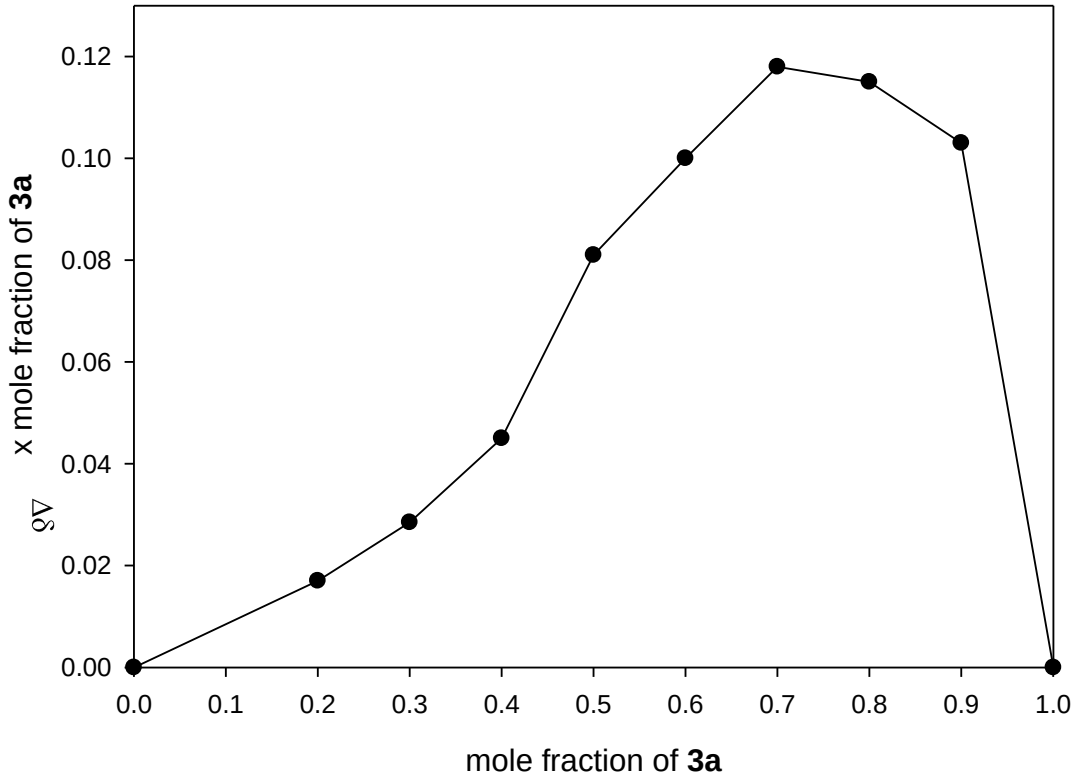

Figure S25. Job plot of macrocycle **3a** with methyl viologen dichloride $\mathbf{7}^{2+}\cdot 2Cl^{-}$ in $CDCl_3/CD_3OD$ (3:1).

Simulations

Given the large size of the macrocycles in this study, their flexibility, and the number of interactions involved (hydrogen-bonding, π-π stacking, electrostatic), detailed DFT calculations were beyond the scope of the study. However, we employed semi-empirical calculations (PM3) to estimate the size of the macrocycles, to determine the expected conformations, and to model the host-guest interactions to correlate with experiments. Calculations were performed on macrocycles **3** using Spartan ’04 for Windows (note that peripheral alkoxy groups were removed for simplification as they are not expected to significantly affect the conformation). Simulations were started from several different likely conformations and minimized from semi-empirical calculations of macrocycles **3**, along with the energies. There may well be additional conformation representing minima on a complex conformational landscape, but these are representative. What they clearly show is that the macrocycle does not have a flat conformation that is conducive to stacking.

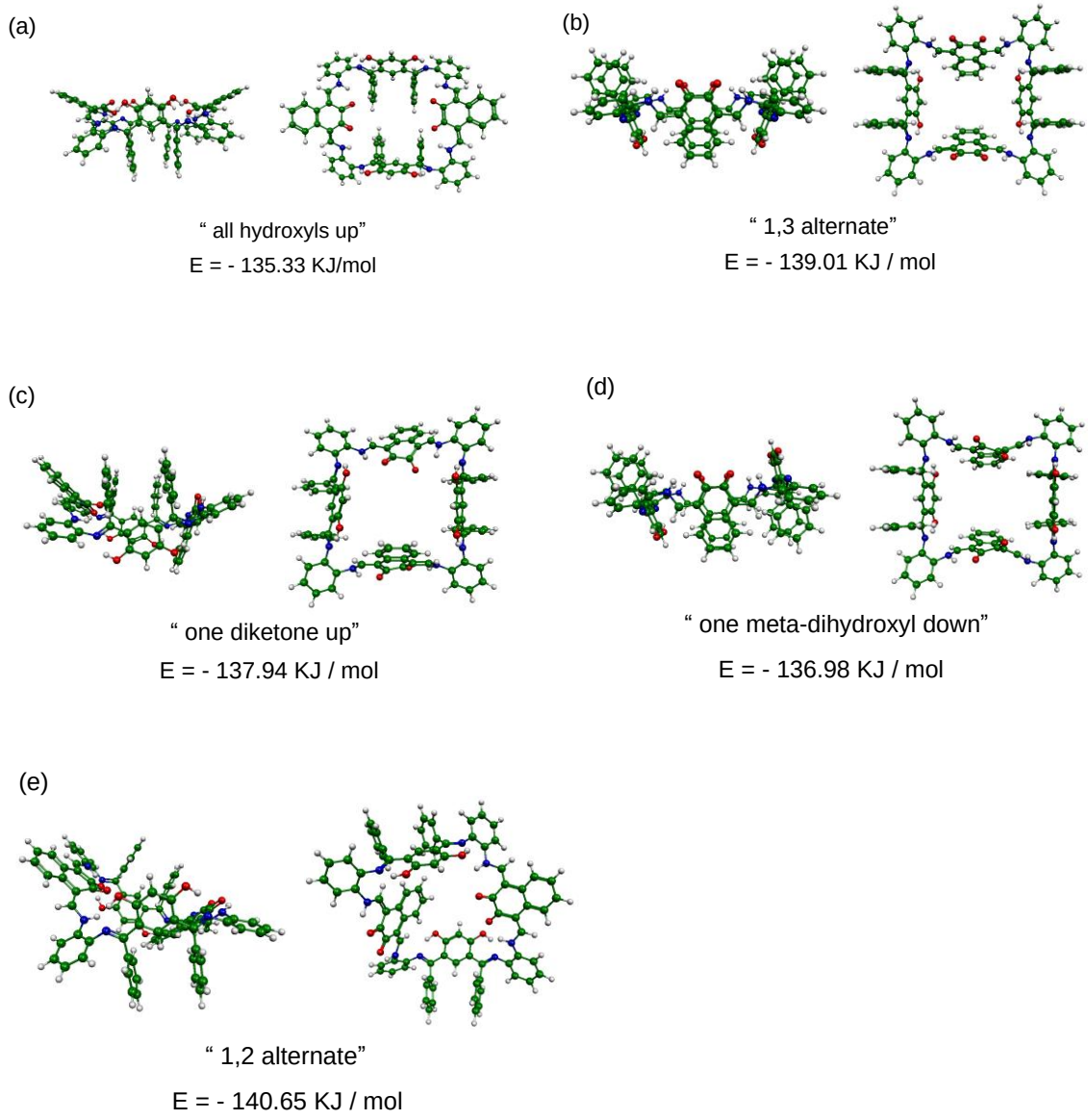

Figure S26. Representative energy-minimized conformations of macrocycle **3a** as deduced by semi-empirical (PM3) measurements. The energy of the conformation is shown beneath each structure. (Nomenclature from calixarene chemistry.)

Energy-minimized structures of the host-guest complexes were examined in a similar way. The guest was incorporated into the interior of the macrocycle starting with different orientations of the guest and different conformations of the host. There are many stable structures as described in the paper. The conformations illustrated in Figure S27 are representative, energy-minimized structures, and do not represent global minima.

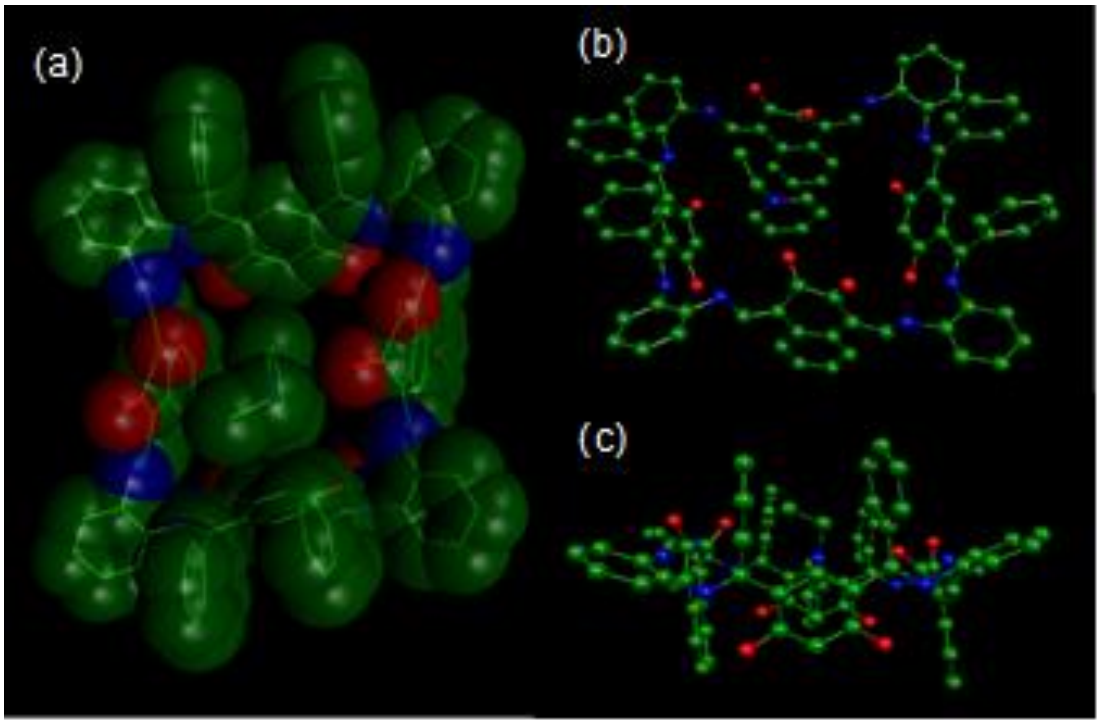

Figure S27. Energy-minimized model of $\mathbf{4}^{+} \subset \mathbf{3a}$ complex (a) space-filling view from bottom; (b) top view; (c) side view. (alkoxy chains of the macrocycle were removed and the alkyl chain of the pyridinium was truncated to ethyl for simplification; protons were removed for clarity.)

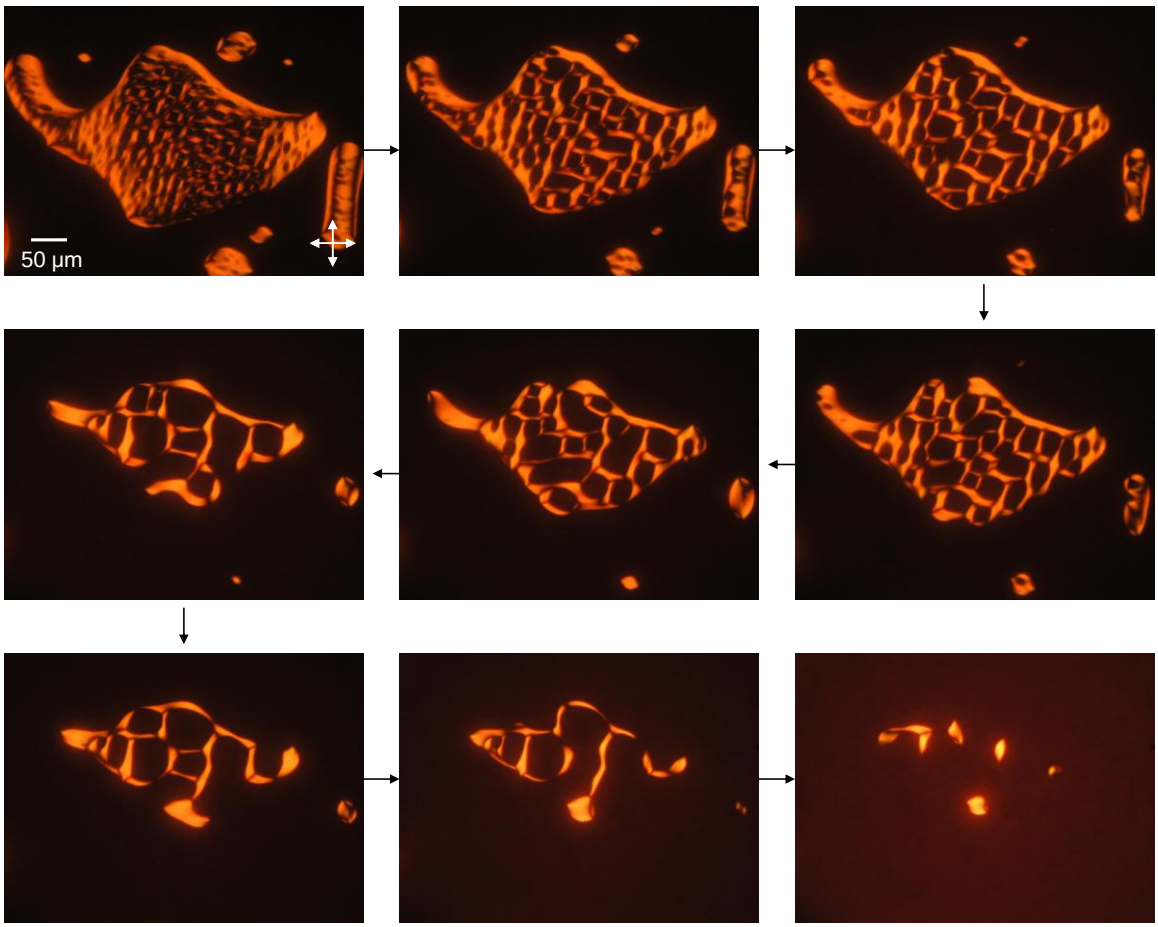

Figure S28. The changes of grid pattern at a high light intensity. (Sequence is indicated by the arrows. The light intensity was fixed at ca. 1100 mW/m^2 at 560 nm)

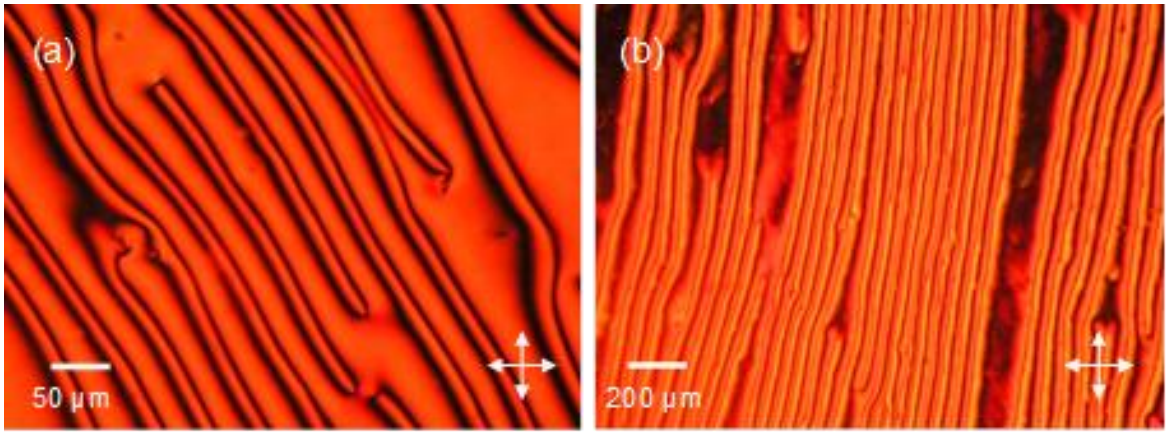

Figure S29. (a), (b) The Schlieren textures of **3b**/chloroform (30 wt% **3b**) sandwiched between untreated glass slides at 22 °C (light intensity of POM is around 200 mW/m^2 at 560 nm).

References

[1] S. Rodriguez-Morales, R. L. Compadre, R. Castillo, P. J. Breen and C. M. Compadre, *Eur. J. Med. Chem.*, 2005, **40**, 840.
[2] P. D. Frischmann, J. Jiang, J. K.-H. Hui, J. J. Grzybowski and M. J. MacLachlan, *Org. Lett.*, 2008, **10**, 1255.
[3] S. Akine, T. Taniguchi and T. Nabeshima, *Tetrahedron Lett.*, 2001, **42**, 8861.
[4] A. J. Gallant, M. Yun, M. Sauer, C. S. Yeung and M. J. MacLachlan, *Org. Lett.*, 2005, **7**, 4827.
[5] J. Jiang and M. J. MacLachlan, *Org. Lett.*, 2010, **12**, 1020.